Spectroscopic Properties of *Escherichia coli* UDP-*N*-Acetylenolpyruvylglucosamine Reductase†

Milton J. Axley,‡ Robert Fairman,§ Joseph Yanchunas, Jr.,§ Joseph J. Villafranca,§ and James G. Robertson*,§

Enzymology Laboratory, Division of Macromolecular Structure, Bristol-Myers Squibb Pharmaceutical Research Institute, Princeton, New Jersey 08543-4000, and Code 512, Naval Medical Research Institute, Bethesda, Maryland 20889

Received September 9, 1996; Revised Manuscript Received November 15, 1996⊗

ABSTRACT: Purified uridine diphosphate *N*-acetylenolpyruvylglucosamine reductase (E.C. 1.1.1.158) was analyzed by circular dichroism (CD) and UV−visible spectroscopy to establish the spectral properties of its tightly bound flavin adenine dinucleotide (FAD) cofactor. The polypeptide backbone displayed a single circular dichroic minimum at 208 nm and a single maximum at 193 nm. The CD spectrum of bound flavin exhibited a single major negative Cotton peak at 364 nm and two minor negative Cotton peaks at 464 and 495 nm. The protein was reversibly unfolded in 9.8 M urea and refolded in buffer in the presence of excess FAD. The refolded enzyme incorporated FAD and catalyzed full activity. The bound FAD displayed an absorption maximum at 464 nm with an extinction coefficient of $\epsilon_{464} = 11700$ M^{-1} cm^{-1}. Anaerobic reduction with dithionite was complete at 1 equiv. Anaerobic reduction with nicotinamide adenine dinucleotide phosphate, reduced form (NADPH), also was essentially complete at 1 equiv and produced a long-wavelength absorbance band characteristic of an FAD−pyridine nucleotide charge transfer complex. Photochemical bleaching in the presence of ethylenediaminetetraacetic acid (EDTA) followed exponential kinetics. None of the anaerobic reductive titrations produced a spectral intermediate characteristic of a flavin semiquinone, and all reduced enzyme species could be fully reoxidized by oxygen, with full recovery of catalytic activity. Photochemically reduced enzyme was reoxidized by titration with either $NADP^+$ or uridine diphospho *N*-acetylglucosamine enolpyruvate (UNAGEP). Reoxidation by $NADP^+$ reached a chemical equilibrium, whereas reoxidation by UNAGEP was stoichiometric. Binding of $NADP^+$ or UNAGEP to the oxidized form of the enzyme produced a dead-end complex that could be titrated by following a 10-nm red shift in the absorption spectrum of the bound FAD. The K_d of $NADP^+$ for oxidized enzyme was 0.7 ± 0.3 μM and the K_d of UNAGEP was 2.7 ± 0.3 μM. Solvent deuterium isotope effects on binding were observed for both $NADP^+$ and UNAGEP, depending on the pH. At pH 8.5, the ${}^{H}K_d/{}^{D}K_d$ was 2.2 for $NADP^+$ and 3.9 for UNAGEP. No spectral changes were observed in the presence of a 40-fold excess of uridine diphospho *N*-acetylmuramic acid (UNAM) either aerobically or anaerobically. These studies have identified spectral signals for five steps in the kinetic mechanism, have indicated that product formation is essentially irreversible, and have indicated that hydrogen bonding or protonation contributes significantly to ground-state complex formation with the physiological substrate.

Uridine diphosphate *N*-acetylenolpyruvylglucosamine reductase (E.C. 1.1.1.158) catalyzes a two-electron reduction of a unique enol ether intermediate in bacterial cell wall biosynthesis, as shown in Figure 1 (Bugg & Walsh, 1993). The enzyme recently has been cloned, overexpressed, and purified and has been shown to contain tightly bound FAD[1] (Benson et al., 1993; Pucci et al., 1992; Dhalla et al., 1995). The chemical mechanism involves NADPH reduction of the bound flavin and subsequent hydride transfer to the vinylic carbon of UNAGEP (Benson et al., 1993). Steady-state kinetic studies have provided evidence for a ping-pong bi-bi double competitive substrate inhibition mechanism (Dhalla et al., 1995). The protein also has been crystallized (Benson et al., 1994), and the crystal structure of the enzyme with and without bound UNAGEP has been solved (Benson et al., 1995, 1996). The structure shows that the polypeptide assembles in three domains that generate a unique fold around the flavin chromophore. The fold does not involve the typical nucleotide binding motif found in many FAD- and NADPH-requiring enzymes.

Kinetic studies indicate that the enzyme is specific for NADPH and is highly specific for UNAGEP as the final electron acceptor (Dhalla et al., 1995). The enzyme also requires a monovalent cation for activation (Dhalla et al., 1995). Crystallographic data suggest that the cation is involved in binding a carboxylate oxygen in the enolpyruvyl moiety (Benson et al., 1995). Nucleotides and sugar nucleotides such as UDP, ADP, ADP-ribose, and UNAG bind only weakly to the enzyme, with K_i s in the range of 5−97 mM (Dhalla et al., 1995). The weak inhibition by

† This research was partially supported by the Naval Medical Research and Development Command, Work Unit Number 61153N. MR04101.001-1508. The opinions and assertions contained herein are the private ones of the authors and are not to be construed as official or reflecting the view of the Navy Department or the naval service at large.

* To whom correspondence should be addressed.

‡ Naval Medical Research Institute.

§ Bristol-Myers Squibb Pharmaceutical Research Institute.

⊗ Abstract published in *Advance ACS Abstracts,* January 15, 1997.

[1] Abbreviations: CD, circular dichroism; EDTA, ethylenediaminetetraacetic acid; FAD, flavin adenine dinucleotide; $NADP^+$, nicotinamide adenine dinucleotide phosphate; NADPH, nicotinamide adenine dinucleotide phosphate, reduced form; UNAG, uridine diphospho *N*-acetylglucosamine; UNAGEP, uridine diphospho *N*-acetylglucosamine enolpyruvate; UNAM, uridine diphospho *N*-acetylmuramic acid.

S0006-2960(96)02260-X CCC: $14.00

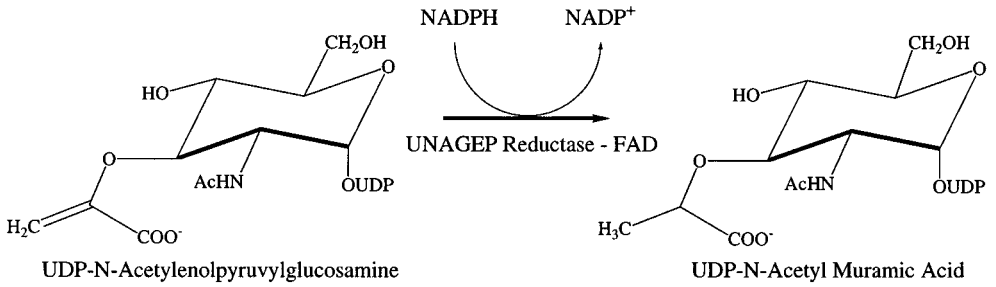

FIGURE 1: Reaction catalyzed by UNAGEP reductase.

UNAG, which does not contain the enolpyruvyl moiety of the substrate, suggests that the enzyme achieves a large degree of specificity through the interactions of the enolpyruvyl moiety with bound FAD or active-site residues.

The proposed ping-pong bi-bi double competitive substrate inhibition mechanism states that each substrate can bind to two forms of the enzyme (Dhalla et al., 1995). In addition, product inhibition patterns show that $NADP^+$ and UNAM also can bind to the enzyme, but with K_is much larger than the K_ms of the substrates. Noncompetitive inhibition by $NADP^+$ with respect to NADPH indicates either that $NADP^+$ can reverse the reaction by reoxidizing reduced flavin or that it can bind to more than one form of the enzyme. In the absence of any direct evidence of $NADP^+$ binding to multiple enzyme forms, its noncompetitive inhibition has been suggested to be due to enzyme reoxidation (Dhalla et al., 1995). Uncompetitive product inhibition by UNAM with respect to NADPH is very weak, with a K_i of 8.4 mM, and any inhibition with respect to UNAGEP could not be measured even at high concentrations of UNAM. Therefore UNAM may bind to multiple enzyme forms but is difficult to study due to the weakness of the interaction.

The kinetic mechanism therefore suggests eight possible binding interactions involving two substrates and two products each binding to two enzyme forms (oxidized and reduced). A minimal microscopic kinetic mechanism should account for at least this many interactions. The present study was conducted to define the available spectral signals that might be used to study each potential binding interaction and to determine the potential significance of hydrogen bonding or protonation on ligand−protein interactions.

MATERIALS AND METHODS

Reagents. Commercially available substrates and product, including FAD, UNAG, NADPH, and $NADP^+$, were from Sigma. Urea, ultrapure grade, was from U.S. Biochemical Corp. Dithionite was from Fluka. Commercial FAD was >97% pure and was used as obtained for determination of the extinction coefficient of enzyme-bound FAD.

Enzyme and Substrate. Enzyme and substrate were prepared as described previously (Dhalla et al., 1995). The standard enzyme assay contained, in a final volume of 1 mL, 50 mM Bis-tris propane, pH 8.0, 50 mM KCl, 125 μM UNAGEP, 150 μM NADPH, and 1 μg of UDP-*N*-acetylenolpyruvylglucosamine reductase. Reaction mixtures without NADPH and enzyme were equilibrated at 37 °C for 10 min. Reactions then were started by sequential addition of NADPH and enzyme.

Determination of Extinction Coefficient of Bound FAD. A solution of known FAD concentration was added to 10 M urea and 50 mM Bis-tris propane, pH 8.0, to determine the extinction coefficient of free FAD in 10 M urea. A value of $\epsilon_{450} = 11\,900\ M^{-1}\ cm^{-1}$ was obtained. The spectrum of native UNAGEP reductase in 50 mM Bis-tris propane was obtained and the peak absorbance at 464 nm was recorded. An identical sample then was unfolded in 10 M urea and 50 mM Bis-tris propane, pH 8.0, and the concentration of released FAD was calculated from its absorbance at 450 nm and the ϵ_{450} of $11\,900\ M^{-1}\ cm^{-1}$. From the known concentration of released FAD and the peak absorbance value of native enzyme at 464 nm, an extinction coefficient of $\epsilon_{464} = 11\,700\ M^{-1}\ cm^{-1}$ was calculated for enzyme-bound FAD. Triplicate samples of free FAD, native enzyme, and unfolded enzyme were used for the determinations, and the results were averaged.

UV−Visible Spectra. Aerobic spectra of UNAGEP reductase were obtained on a Cary 3E spectrophotometer. Scans were obtained with a spectral bandwidth of 2 nm, at 0.5-nm increments, and with a 1-s averaging time. Anaerobic spectra were obtained on an HP 8452 diode array spectrophotometer placed in an anaerobic chamber from Coy Laboratories (Ann Arbor, MI). The chamber was maintained under an atmosphere of 5% hydrogen and 95% nitrogen, and oxygen content was monitored continuously by a gas analyzer (Coy Laboratories). An oxygen scrubbing system in the chamber maintained the oxygen concentration below detectable limits (<1 ppm) during daily passage of material into the chamber through the airlock.

Anaerobic buffers were kept in the chamber, and solutions of substrates, products, and enzyme were passed into the chamber and equilibrated with the atmosphere for at least an hour before use. Concentrated solutions of enzyme and ligands then were diluted into anaerobic buffer for use in spectral titrations. Solutions of dithionite were prepared in 100 mM Bis-tris propane, pH 8.0, and were standardized by titration against a known amount of FAD. Enzyme solutions at 25 °C in 2-mL volumes were titrated with ligand solutions delivered from a 10-μl Hamilton syringe attached to a repeating dispenser measuring 0.2-μL volumes. For anaerobic photochemical reduction, cuvettes containing enzyme and 50 mM EDTA were placed 1 cm from a 50-W fluorescent bulb in the anaerobic chamber and were exposed for the times indicated in the figure legends.

Aerobic titrations with $NADP^+$ and UNAGEP were conducted in a Cary 3E spectrophotometer at 20 °C in buffers prepared in either H_2O or D_2O. Buffers contained final concentrations of 50 mM Bis-tris propane and 50 mM KCl at the specified pH. Buffer in D_2O was adjusted to the final pH with either DCl or KOD, and the specified pD values in Figure 11 equal the pH + 0.4. For the experiments in Figure 11, cuvettes containing 1700 μL of buffer and KCl were equilibrated at 20 °C for 10 min, and then 100 μL of enzyme

solution was added. The titrations then were performed with a 10-μL Hamilton syringe attached to a repeating dispenser measuring 0.2-μL volumes. The final D_2O concentration was 94%.

Circular Dichroism. Circular dichroic spectra were obtained on an Aviv Model 62DS instrument. Native enzyme was equilibrated in 1 mM Na_2HPO_4, pH 8.0, by chromatography on a PD10 column. The final concentration of equilibrated enzyme was 30 μM. An aliquot of 30 μM enzyme was diluted with H_2O to 1.5 μM. The spectrum of 1.5 μM native enzyme was obtained in a 0.1-cm path length cell at 25 °C with a step size of 0.25 nm. For the top panel in Figure 2, data were collected with signal averaging of 5 s/point, and 25 spectra were averaged. For the data in the bottom panel of Figure 2, the CD spectrum of bound FAD, a sample of native enzyme was desalted on a PD10 column, dialyzed overnight against 1 mM Na_2HPO_4, pH 8.0, and then concentrated to 200 μM in a Centricon 30. Data were collected in a 0.5-cm path length cell with signal averaging of 5 s/point and 1-nm step size, and 10 spectra were averaged. Scans of 1 mM Na_2HPO_4, pH 8.0, were subtracted as blanks. Estimates of the secondary structure were obtained by fitting to a basis set of 33 proteins as previously described (Manavalan & Johnson, 1987). Secondary structural predictions were obtained from the Chou−Fasman algorithm implemented in GeneWorks from IntelliGenetics or from a neural net algorithm as described previously (Rost & Sander, 1993, 1994).

For CD spectra of unfolded protein and reconstituted enzyme, as shown in the inset of Figure 2, the enzyme was denatured and refolded as described below. The CD spectra of denatured protein were obtained at a concentration of 4.5 mg/mL protein in 20 mM Bis-tris propane containing 9.8 M urea and 10 mM dithiothreitol. Spectra were obtained in a 0.001-cm path length cell with a 0.25-nm step size and 2 s/point averaging, and 5 scans were averaged. Spectra of renatured protein were obtained as described above in 1 mM Na_2HPO_4, pH 8.0.

Anaerobic Circular Dichroism. Enzyme samples were made anaerobic in sealed Thunberg-type cuvettes with a side arm and tapered seal to a stopcock. Samples were alternately evacuated and flushed with argon for at least 30 min. The sealed cuvettes in a final argon atmosphere were transferred to an Aviv Model 62DS spectrophotometer, and the sample compartment was flushed with a continuous stream of nitrogen. Reactions contained, in a final volume of 2 mL, 50 mM Bis-tris propane, pH 8.0, 30 μM enzyme, and the concentrations of reductants or ligands shown in the figure legends. Reduction with NADPH and photochemical reduction in the presence of 50 mM EDTA were performed anaerobically. The completeness of reduction was assessed by overlap of CD spectra taken as a function of time. As a result of this, each spectrum shown represents averaging of 2−4 individual spectra. Visible CD spectra were obtained using a 1.0-cm cell, a 0.5-cm step size, a 1.0-s averaging time, and a bandwidth of 1.2 nm. Spectra with UNAGEP or $NADP^+$ bound were obtained under aerobic conditions (open cuvettes) and the spectrum with excess dithionite also was obtained under aerobic conditions (open cuvettes). Controls with FAD (20 μM) or UNAGEP (300 μM) alone demonstrated no observable CD signals.

Enzyme Denaturation−Renaturation. Denatured enzyme was prepared by dissolving solid urea in 5.4 mL of 13 mg/mL enzyme. The final solution contained 20 mM Bis-tris propane, pH 8.0, 10 mM dithiothreitol, and 9.8 M urea. To remove FAD, the sample was desalted on a Sephadex G-25 column equilibrated in buffer containing 9.8 M urea and 10 mM dithiothreitol. Protein from the desalting column was pooled and quantitated by absorbance at 280 nm using an extinction coefficient of 51 350 M^{-1} cm^{-1} calculated from the tyrosine and tryptophan content (Edelhoch, 1967). The concentration of recovered material was 4.5 mg/mL. The CD spectrum of 4.5 mg/mL protein in 9.8 M urea was obtained, as shown in Figure 2. Subsequently, one aliquot was diluted to 0.6 mg/mL in 20 mM Bis-tris propane containing 9.8 M urea and 10 mM dithiothreitol, and the UV−visible spectrum was obtained, as shown in Figure 3. After denaturation and chromatography, 41 mg of protein was recovered from the 70 mg of starting material.

Solid FAD was added to 9 mL of denatured protein to give a final concentration of 1 mM, and the protein solution in 20 mM Bis-tris propane, 9.8 M urea, and 10 mM dithiothreitol was dialyzed at 4 °C against 100 mL of buffer containing 10 mM Bis-tris propane, pH 8.0, and 10 mM dithiothreitol. After 24 h, the sample was dialyzed against two changes of 100 mL of 10 mM Bis-tris propane, pH 8.0, 100 μM FAD, and 10 mM dithiothreitol for 12 h each. The sample then was dialyzed for 24 h against 100 mL of 10 mM Bis-tris propane, pH 8.0, 10 μM FAD, and 10 mM dithiothreitol.

The recovered sample was concentrated to 2 mL in a Centriprep 30 and was washed twice with 15 mL of 10 mM Bis-tris propane, pH 8.0. The concentrated sample then was desalted on a PD10 column containing 50 mM Bis-tris propane, pH 8.0. The recovered protein was quantitated by FAD absorbance at 464 nm using an extinction coefficient of 11 700 M^{-1} cm^{-1}. The final recovery of folded enzyme was 24%. The refolded enzyme had a specific activity of 60 units/mg at 37 °C. A sample of refolded enzyme was equilibrated in 1 mM Na_2HPO_4, pH 8.0, and the CD spectrum was obtained as described above and is shown in Figure 2.

Data Analysis. Kinetic parameters were determined by fitting to eqs 1 and 2 by nonlinear regression. Binding curves were fitted to the quadratic expression for a single binding equilibrium under conditions where the free ligand concentration changes substantially during the titration (eq 3), where A is the measured absorption, A_o is the starting absorption, ΔA is the total measured change in absorption, E_o is the enzyme concentration, K_d is the ligand dissociation constant, and S_o is the concentration of ligand added to the enzyme (Anderson et al., 1988). Ligand binding stoichiometries were determined by fixing the enzyme concentration at 1 or 2 times the known enzyme concentration (from the flavin absorbance) during the fitting process. Saturation plots could not be fitted to a model representing twice the known concentration of enzyme, and therefore a stoichiometry of 2 could be eliminated.

$$v = (V_m S)/(K_m + S) \quad (1)$$

$$v = (V_m S)/(K_m + S + S^2/K_i) \quad (2)$$

$$A = A_0 + (\Delta A/E_0)\{(K_d + [E_0] + [S_0]) - [(K_d + [E_0] + [S_0])^2 - 4[E_0][S_0]]^{1/2}\}/2 \quad (3)$$

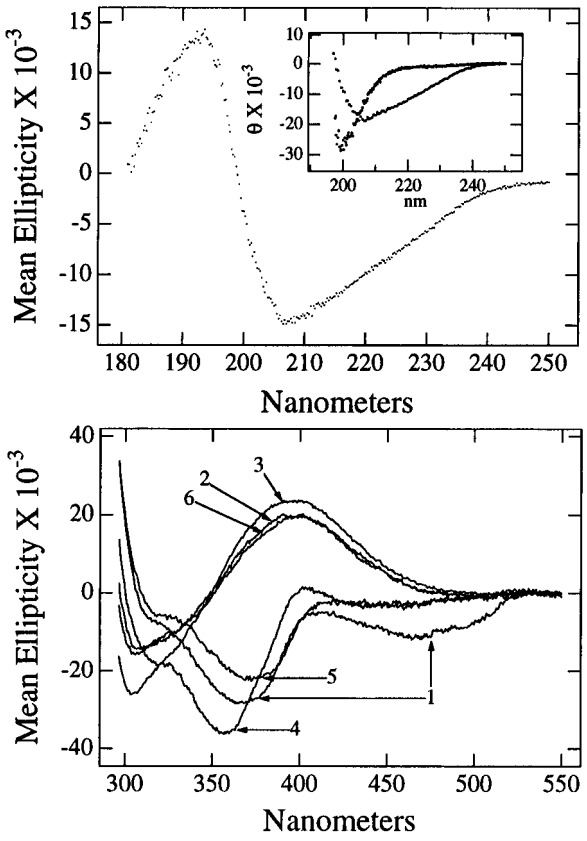

FIGURE 2: Circular dichroic spectra of native UNAGEP reductase. The spectrum of 1.5 μM (0.06 mg/mL) native enzyme (top panel) in 1 mM Na_2HPO_4, pH 8.0, was obtained in a 0.1-cm path length cell at 25 °C, as described under Materials and Methods. The visible CD spectra in the bottom panel were obtained as described under Materials and Methods at 30 μM enzyme and the following concentrations: 1 = no addition, 2 = 200 μM NADPH, 3 = 600 μM dithionite, 4 = 300 μM UNAGEP, 5 = 300 μM $NADP^+$, and 6 = 50 mM EDTA and 90 min of exposure to fluorescent light. Spectra 2 and 6 were obtained in sealed cuvettes under anaerobic conditions. The inset to the top panel shows the circular dichroic spectra of denatured and renatured UNAGEP reductase. Enzyme was denatured and renatured as described under Materials and Methods. The circular dichroic spectrum of denatured enzyme was obtained at a concentration of 117 μM (4.5 mg/mL) enzyme in 20 mM Bis-tris propane, pH 8.0, 9.8 M urea, and 10 mM dithiothreitol, in a 0.001-cm path length cell. The spectrum of renatured enzyme was obtained at a protein concentration of 1.5 μM (0.06 mg/mL) in 1 mM Na_2HPO_4, pH 8.0, in a 0.1-cm path length cell. Both spectra were obtained at 25 °C, and the corresponding buffer blanks were subtracted from each spectrum. The spectrum with a minimum at 200 nm corresponds to denatured enzyme, and the spectrum with a minimum at 208 nm represents renatured enzyme.

RESULTS

CD Spectra. Circular dichroic spectra of native enzyme were obtained to estimate the relative amounts of sheets and helices in UNAGEP reductase. Figure 2, top panel, shows the spectrum of native enzyme in dilute phosphate buffer at pH 8.0. The spectrum of the polypeptide displayed a single minimum at 208 nm and a single maximum at 193 nm. The spectrum of the polypeptide from 181 to 250 nm was fitted to a basis set of 33 proteins (Manavalan & Johnson, 1987), and Table 1 lists the relative amounts of structural elements estimated by this procedure. Table 1 also lists the structural elements predicted by sequence analysis using two different algorithms and the structural elements predicted by analysis of the hydrogen-bonding patterns in the crystal structure (Kabsch & Sander, 1983). The predictive algorithms and CD analysis showed general agreement on the percentage of helix and strand known to be in the crystal structure.

Table 1: Secondary Structure of UNAGEP Reductase

secondary structure	method or type of measurement			
	CD	Chou−Fasman	neural net	crystal structure
helix (%)	24	27	29	22
strand (%)	23[a]	29	22	23
turn (%)	24	33		24
loop (%)			49[b]	
other (%)	31			
total (%)	102	89	100	69[c]

[a] The CD deconvolution algorithm reports the percentage of antiparallel and parallel β sheet. The percent strand reported for this algorithm is the sum of these two values. [b] The neural net algorithm reports the percentage of all structure other than helix and strand as loop. [c] Analysis of the secondary structure in the crystal structure was performed using the algorithm in Kabsch and Sander (1983), which only reports the relative amounts of helix, strand, and turn.

Visible CD spectra of oxidized and reduced enzyme also were obtained for comparison to the absorbance spectra. The CD spectrum of oxidized flavin exibited a single major negative Cotton peak at 366 nm and two minor negative Cotton peaks at 469 and 495 nm, as shown in Figure 2, bottom panel. These closely agreed with the visible peaks in the absorption spectrum (see below) . The spectrum of fully reduced enzyme was obtained aerobically with excess dithionite, and anaerobically with excess NADPH, and anaerobically by photochemical reduction in the presence of EDTA. The reduced enzyme displayed a positive Cotton peak at 396 nm with each method of reduction.

Interestingly, aerobic addition of $NADP^+$ or UNAGEP resulted in CD spectra that are remarkably different from either the reduced or fully oxidized form. Binding of $NADP^+$ eliminates the negative Cotton peak at 464 nm and red-shifts the peak at 364 nm to 372 nm. Similarly, binding of UNAGEP eliminates the peak at 464 nm, but intensifies and blue-shifts the peak at 364 nm to 357 nm. These changes suggest that the substrate and product might have an effect on the redox potential of the flavin (Edmondson & Tollin, 1971).

Figure 2, top panel, inset, shows the CD spectra of denatured enzyme in 9.8 M urea and renatured enzyme in 1 mM phosphate buffer at pH 8.0. The spectrum in 9.8 M urea illustrates the conversion to random coil in the denatured state, with a minimum at 200 nm, and the spectrum of refolded protein in phosphate buffer demonstrates the recovery of native structure with a single minimum at 208 nm.

UV−Visible Spectra of Native and Reconstituted Enzyme. Figure 3 shows the spectrum of native enzyme, denatured enzyme after removal of FAD, and enzyme renatured in the presence of FAD. Native enzyme displayed absorption maxima at 273, 374, and 464 nm and a pronounced shoulder at 495 nm. The A_{280}/A_{466} ratio was 8.1. The results are similar to those published previously (Dhalla et al., 1995). After denaturation in 9.8 M urea and chromatography on a Sephadex G-25 column to remove FAD, the protein displayed a single major peak at 280 nm. In order to renature the enzyme, UNAGEP reductase was dialyzed slowly in the presence of excess FAD and dithiothreitol to remove urea and reincorporate flavin. Each of the major peaks was present in renatured enzyme, and renatured enzyme displayed

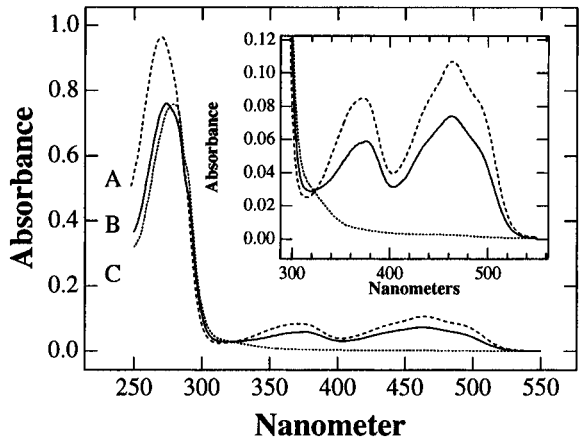

FIGURE 3: UV−visible spectra of native, denatured, and renatured UNAGEP reductase. Enzyme was denatured and renatured as described under Materials and Methods. The spectrum of native enzyme (A, - - -) was obtained in 50 mM Bis-tris propane, pH 8.0, at a concentration of 9 μM (0.35 mg/mL). The spectrum of denatured and desalted enzyme (C, ···) was obtained in 20 mM Bis-tris propane containing 9.8 M urea and 10 mM dithiothreitol, at a protein concentration of 16 μM (0.6 mg/mL). The spectrum of renatured enzyme (B, —) was obtained in 50 mM Bis-tris propane, pH 8.0, at a concentration of 6 μM (0.24 mg/mL). All spectra were obtained on a Cary 3E spectrophotometer at 25 °C.

full catalytic activity. The extinction coefficient of bound FAD was determined to be $\epsilon_{464} = 11\,700$ M^{-1} cm^{-1}, as described under Materials and Methods.

Substrate and Product Binding to Oxidized Enzyme. Enzyme was titrated separately with UNAGEP, UNAM, NADPH, and $NADP^+$ under aerobic conditions to determine whether or not there are detectable spectral changes upon ligand binding to oxidized enzyme. Experiments demonstrated that NADPH transiently reduces the enzyme but that in the presence of oxygen the reduced FAD reoxidizes in a matter of seconds. Preliminary experiments also demonstrated that there were no changes in the UV−visible spectrum of bound FAD in the presence of up to 2 mM UNAM.

In contrast, both UNAGEP and $NADP^+$ red-shifted the absorbance maximum at 464 nm to a new maximum at 474 nm when they were added to aerobic solutions of enzyme. The shift could be quantitated by measuring the absorbance increase at 510 nm in a region of the spectrum displaying the greatest absorbance change. This red shift also was observed during titration with UNAGEP or $NADP^+$ under anaerobic conditions.

Figure 4 illustrates the spectral shift due to UNAGEP binding. The peak shift produced a new maximum at 474 nm and three isosbestic points at 380, 410, and 470 nm. The peak shift also produced a new maximum at 380 nm and a new minimum at 412 nm. The new maximum at 380 nm had a lower extinction coefficient, and the new minimum at 410 nm had a higher extinction coefficient, than the corresponding maximum and minimum of free enzyme. Under these conditions, UNAGEP binding represents the formation of a dead-end complex because there are no reducing equivalents present for reduction of the olefinic bond in the substrate. The ligand bound with a K_d of 2.7 ± 0.3 μM and a stoichiometry of 1. The K_m under similar conditions was 2.2 ± 0.3 μM, as shown in Table 2.

Similarly, Figure 5 illustrates the spectral shift due to $NADP^+$ binding. The peak shift produced a new maximum

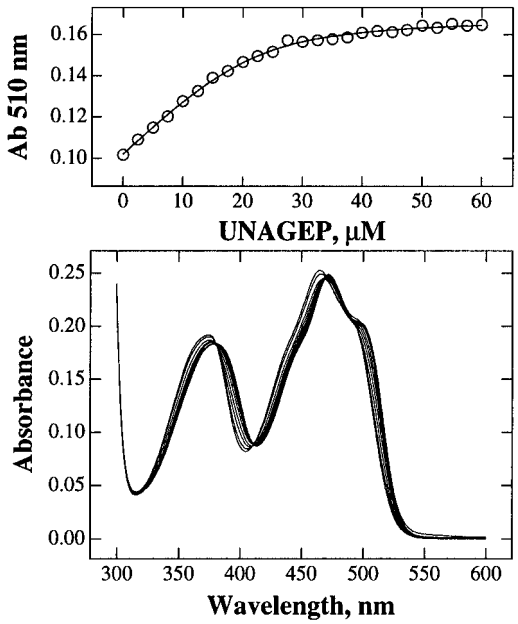

FIGURE 4: Aerobic titration of UNAGEP reductase with UNAGEP. Enzyme was titrated as described under Materials and Methods. The spectrum of free enzyme was obtained in 50 mM Bis-tris propane, pH 8.0, and 50 mM KCl, at a concentration of 24 μM (0.9 mg/mL) in a 2-mL volume. Ligand was titrated to a final concentration of 60 μM in 0.2-μL increments using a repeating dispenser and a 10-μL gas-tight glass syringe (bottom panel). Every other spectrum is shown for clarity. The absorbance change at 510 nm was plotted as a function of UNAGEP concentration (top panel), and data were fitted to eq 3. All spectra were obtained on a Cary 3E spectrophotometer at 20 °C.

Table 2: Binding and Kinetic Parameters for UNAGEP Reductase[a]

k_{cat}	14 ± 1.9 s^{-1}
$K_{m,NADPH}$	17 ± 4.9 μM
$K_{m,UNAGEP}$	2.2 ± 0.3 μM
$K_{i,UNAGEP}$	880 ± 160 μM
$K_{d,NADP+}$ for E_{ox}	0.7 ± 0.3 μM
$K_{d,UNAGEP}$ for E_{ox}	2.7 ± 0.3 μM

[a] Kinetic assays were performed as described in Materials and Methods, except that the temperature was 20 °C. Data for NADPH saturation were fitted to eq 1, and data for UNAGEP saturation were fitted to eq 2. The binding constants are from the data in Figures 4 and 5.

at 474 nm and three isobestic points at 378 nm, 406, and 471 nm. The peak shift also produced a new maximum at 384 nm and a new minimum at 414 nm. The new maximum at 384 nm had a higher extinction coefficient, and the new minimum at 410 nm had a lower extinction coefficient, than the corresponding maximum and minimum of free enzyme. Under these conditions, $NADP^+$ binding also represents the formation of a dead-end complex between $NADP^+$ and oxidized enzyme because there are no further chemical steps possible. The ligand bound with a K_d of 0.7 ± 0.3 μM and a stoichiometry of 1.

The spectra in Figures 4 and 5 show that the isosbestic points in the two titrations are slightly different in the 378−380-nm and 406−410-nm regions and that the extinction coefficients shift in opposite directions in the same regions. These small differences indicate that the environment around the flavin may be slightly different in the two bound forms of oxidized enzyme. This is consistent with the CD data in Figure 2 that also show small differences in the two bound forms of oxidized enzyme.

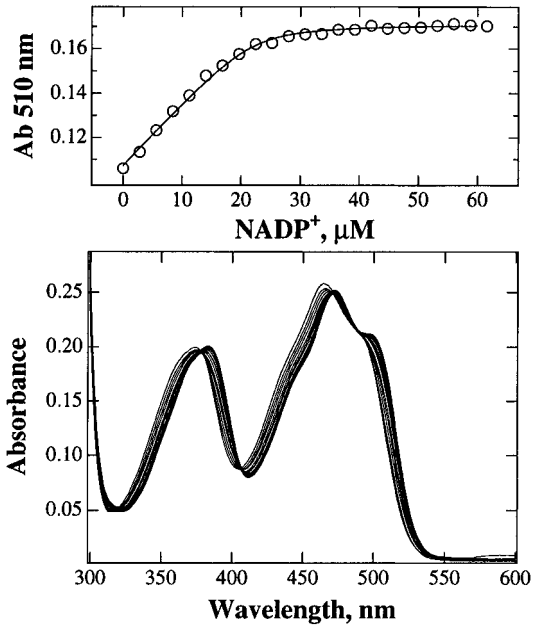

FIGURE 5: Aerobic titration of UNAGEP reductase with $NADP^+$. Enzyme was titrated as described under Materials and Methods. The titration and analysis were the same as in Figure 4 except that $NADP^+$ was the ligand and the final ligand concentration was 62 μM.

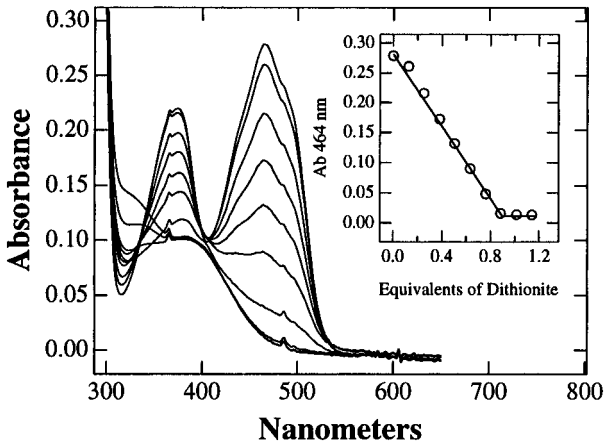

FIGURE 6: Anaerobic reduction of UNAGEP reductase with dithionite. Enzyme was prepared anaerobically in a glove box and titrated with dithionite as described under Materials and Methods. Conditions and procedures were as in Figure 4. Dithionite was titrated to a final concentration of 30 μM. The absorbance change at 464 nm was plotted as a function of dithionite equivalents (inset). All spectra were obtained on a HP 8452 diode array spectrophotometer at 25 °C.

Anaerobic Reduction of Bound FAD by Dithionite. Enzyme containing oxidized FAD was made anaerobic by equilibration under an atmosphere of 5% hydrogen and 95% nitrogen, as described under Materials and Methods. The bound flavin then was reduced with dithionite, as shown in Figure 6. Reduction proceeded in a single phase and was complete with 1 equiv of dithionite. No intermediate spectra with long-wavelength bands were observed during the titration. Dithionite reduction produced an isosbestic point at 408 nm for the first 0.6 equiv, and thereafter the spectra did not converge. At 1 equiv, the peak absorbance at 464 nm was reduced to <5% of the initial value. Exposure to air resulted in reoxidation of the enzyme, and the spectrum of reoxidized enzyme was identical to that of the starting

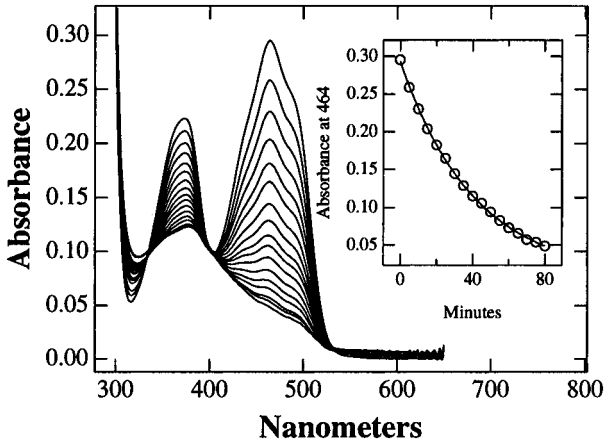

FIGURE 7: Anaerobic photochemical reduction of UNAGEP reductase. Enzyme was prepared anaerobically in a glove box and was exposed to fluorescent light as described under Materials and Methods. Conditions and procedures were as in Figure 4. Spectra were recorded every 5 min during photochemical reduction. Every other spectrum is shown for clarity. The absorbance change at 464 nm was plotted as a function of time (inset), and data were fitted to a single exponential. All spectra were obtained on a HP 8452 diode array spectrophotometer at 25 °C.

spectrum. The reoxidized enzyme also demonstrated full catalytic activity.

Anaerobic Photochemical Reduction of Bound FAD. Oxidized enzyme was reduced under anaerobic conditions by photochemical reduction in the presence of EDTA, as shown in Figure 7. Exposure to fluorescent light for 90 min produced a reduced enzyme species with a minimum at 464 nm, and no intermediate spectra with significant long-wavelength absorbance bands were observed during the reduction. The long-wavelength absorbance band above 550 nm may indicate the presence of small amounts of one-electron-reduced, blue semiquinone. However, the low intensity indicates that such a potential species does not accumulate in significant amounts. Reduction followed an exponential time course, and no further reduction was observed after 90 min under the conditions used. The final absorbance at 464 nm was 16% of the starting value. Air-reoxidized enzyme demonstrated full recovery of the oxidized spectrum and full catalytic activity.

Anaerobic Reduction of Bound FAD by NADPH. Oxidized enzyme also was reduced under anaerobic conditions by titration with NADPH, as shown in Figure 8. Reduction of the absorbance at 464 nm was linear up to approximately 1 equiv of NADPH, and the reduction produced two isosbestic points at 408 and 536 nm. During the titration, the peak at 464 nm shifted to 472 nm, which is characteristic of $NADP^+$ binding, as shown in Figure 5. The final absorbance at 464 nm was 12% of the initial value. Reduction by NADPH also produced featureless long-wavelength absorbance above 536 nm. Appearance of the long-wavelength absorbance followed hyperbolic saturation kinetics, as shown in Figure 8. The long-wavelength absorbance may indicate the formation of a charge transfer complex between the pyridine nucleotide and bound FAD. As above, air-reoxidized enzyme demonstrated full recovery of the oxidized spectrum and full catalytic activity.

Reoxidation of Anaerobically Photochemically Reduced Enzyme by UNAGEP and $NADP^+$. Anaerobic enzyme photochemically reduced in the presence of EDTA was used to measure reoxidation by $NADP^+$ and UNAGEP. As shown

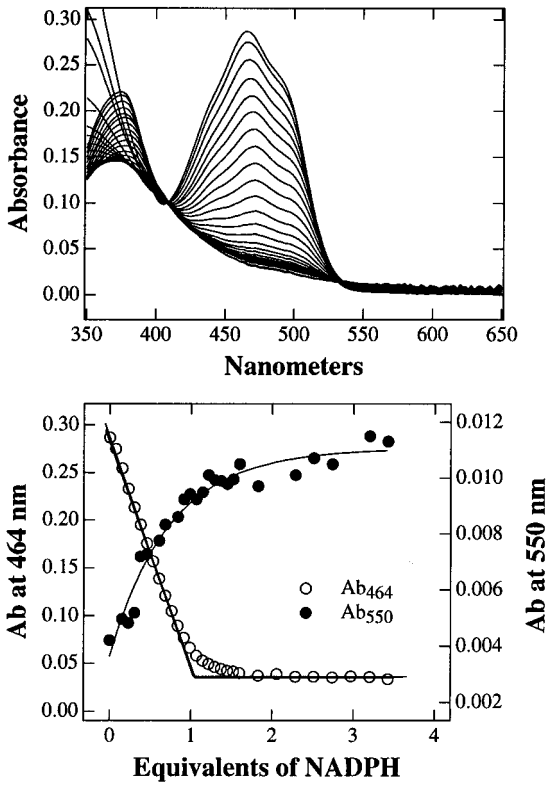

FIGURE 8: Anaerobic reduction of UNAGEP reductase with NADPH. Enzyme was prepared anaerobically in a glove box and was titrated with NADPH as described under Materials and Methods. Conditions and procedures were as in Figure 4. Additions of NADPH were made to a final concentration of 150 μM (top panel). The absorbance changes at 464 and 520 nm were plotted as a function of NADPH equivalents (bottom panel). All spectra were obtained on a HP 8452 diode array spectrophotometer at 25 °C.

in Figure 9, enzyme that was photochemically reduced to 18% of its initial value at 464 nm could be partially reoxidized by titration with $NADP^+$. Addition of $NADP^+$ to reduced enzyme caused a red shift of the 464-nm peak to 474 nm and resulted in a pronounced shoulder at 510 nm. The spectrum of partially reoxidized enzyme was very similar to the spectrum of oxidized enzyme titrated with $NADP^+$. However, a large excess of $NADP^+$ was required for reoxidation, and chemical equilibrium was reached at only 63% of the maximum absorbance of oxidized enzyme at 464 nm. Reoxidation with $NADP^+$ did not produce an isosbestic point in the titration. The plot of absorbance at 474 nm versus equivalents of $NADP^+$ was not exactly hyperbolic and was best fitted to a single exponential. This reflects the fact that the observed potential of the flavin follows Nernstian behavior, which is a logarithmic function of $[FAD_{ox}]/[FAD_{red}]$. Comparison of Figures 8 and 9 suggests that the potential under these conditions favors reduction of the flavin, since reduction is essentially stoichiometric and reoxidation by $NADP^+$ is incomplete even at >25 equiv.

In contrast, when anaerobic, photochemically reduced enzyme was used to measure reoxidation by UNAGEP, reoxidation was stoichiometric, as shown in Figure 10. Starting with enzyme reduced to 20% of its initial value at 464 nm, addition of 0.8 equiv of UNAGEP produced fully oxidized enzyme. Moreover, excess equivalents of UNAGEP over enzyme began to produce a slight red shift of the 464-nm peak identical to that observed in Figure 4, which indicates binding of excess UNAGEP to oxidized enzyme.

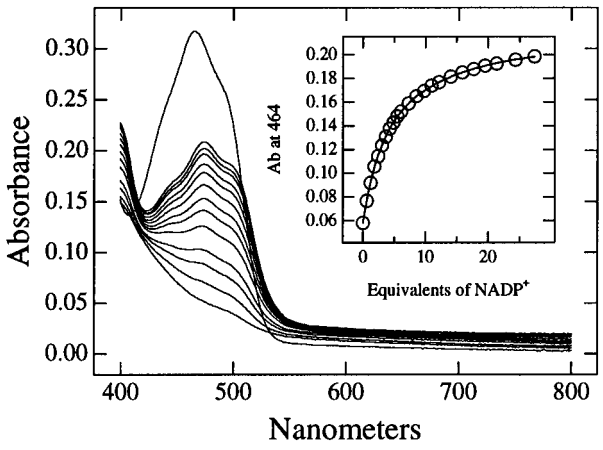

FIGURE 9: Anaerobic reoxidation of photochemically reduced UNAGEP reductase with $NADP^+$. Enzyme was prepared anaerobically in a glove box and was photochemically reduced as described under Materials and Methods. Conditions and procedures were as in Figure 4. Starting absorbance at 464 nm was 0.317. Photochemical reduction was carried out for 120 min, at which time the absorbance at 464 nm was 0.057, or 18% of its starting value. At this point, $NADP^+$ was added to reduced enzyme to a final concentration of 740 μM. The absorbance increase at 464 nm was plotted as a function of $NADP^+$ concentration (inset), and data were fitted to a single-exponential increase. Every other spectrum is shown for clarity. All spectra were obtained on a HP 8452 diode array spectrophotometer at 25 °C.

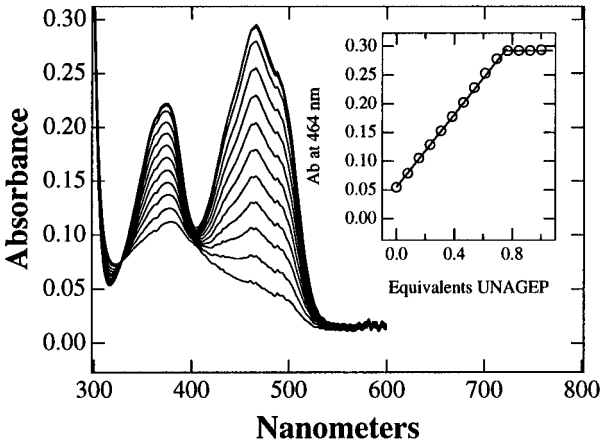

FIGURE 10: Anaerobic reoxidation of photochemically reduced UNAGEP reductase with UNAGEP. Enzyme was prepared anaerobically in a glove box and was photochemically reduced as described under Materials and Methods. Conditions and procedures were as in Figure 4. Photochemical reduction was carried out for 90 min. At this time, UNAGEP was added to reduced enzyme to a final concentration of 26 μM. The absorbance increase at 464 nm was plotted as a function of UNAGEP equivalents (inset). All spectra were obtained on a HP 8452 diode array spectrophotometer at 25 °C.

The stoichiometric reoxidation observed in Figure 10, and the lack of any observable flavin reduction in the presence of 2 mM UNAM (see above), indicates that the chemical equilibrium is essentially irreversible in the direction of UNAM formation.

Solvent Deuterium Isotope Effect on UNAGEP and $NADP^+$ Binding. The experiments in Figures 4 and 5 were repeated in triplicate in H_2O or D_2O to determine whether or not there are any solvent deuterium isotope effects on ligand binding. Also, the binding experiments were conducted at three pH (pD) values to determine the ionization dependence of the isotope effects. As shown in Figure 11 and Table 3, binding of UNAGEP in D_2O was stronger at

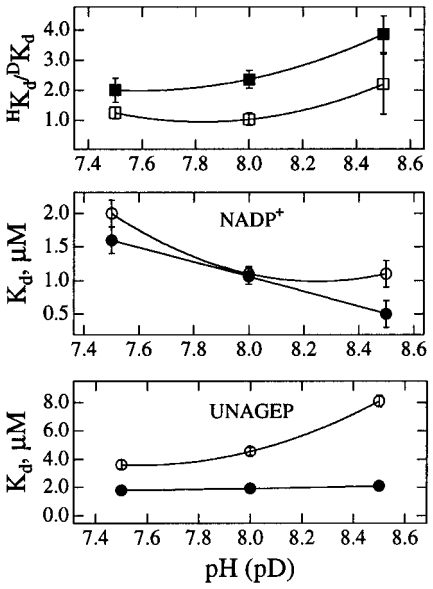

FIGURE 11: pH dependence of $NADP^+$ and UNAGEP binding constants in H_2O and D_2O. Enzyme was titrated as described above in Figures 4 and 5, at a concentration of 7 μM (0.3 mg/mL) in a 1.8-mL volume at pH 7.5, 8.0, and 8.5. Triplicate titrations were done in H_2O and then in D_2O on the same day with the same enzyme sample. The absorbance change at 510 nm was plotted as a function of ligand concentration, and data were fitted to eq 3. All titrations were performed on a Cary 3E spectrophotometer at 20 °C. Open circles (○) represent the K_ds obtained in H_2O, and closed circles (●) represent the K_ds obtained in D_2O. Open squares (□) represent the $^{H}K_d/^{D}K_d$ ratio for $NADP^+$, and closed squares (■) represent the $^{H}K_d/^{D}K_d$ ratio for UNAGEP. Error bars for the $^{H}K_d/^{D}K_d$ ratio were determined from the SE of the individual K_ds by the method in Fieller (1954).

each pH than binding of UNAGEP in H_2O. The $^{H}K_d/^{D}K_d$ ratios ranged from 2 to 3.9. For $NADP^+$, there was little or no solvent deuterium isotope effect, depending on the pH (pD). In D_2O, the binding constant decreased from 1.6 to 1.06 to 0.5 μM as the pD was increased from 7.5 to 8.0 to 8.5. In H_2O, the binding constant decreased from 2.0 to 1.1 to 1.1 as the pH was increased from 7.5 to 8.0 to 8.5. Thus there was essentially no solvent deuterium isotope effect on binding at pH (pD) 7.5 and 8.0, but at pH (pD) 8.5 there was a measurable effect, as shown in Figure 11, though the estimation of $^{H}K_d/^{D}K_d$ contained significant error as a result of propagation of the standard error in the individual K_d s.

DISCUSSION

Flavoenzymes have been classified according to reaction type into five major groups, including transhydrogenases, oxygenases, oxidases, one-electron transferases, and two-electron transferases (Massey & Hemmerich, 1980). The transhydrogenases are further divided into four subclasses, depending on the heteroatoms involved in electron transfer. The reaction catalyzed by UNAGEP reductase falls into the carbon−carbon transhydrogenase subclass. In general, these enzymes catalyze two-electron transfers between nicotinamide nucleotides and acyl or enoyl functionalities, as well as between different nicotinamide nucleotides. In UNAGEP reductase, the transfer is from NADPH to the vinylic bond of UDP-*N*-acetylenolpyruvylglucosamine.

The enzyme demonstrated reversible folding, as shown by the CD and UV-visible spectra in Figures 2 and 3. The renatured enzyme had full catalytic activity and showed a flavin spectrum identical to that of the native enzyme prior to unfolding. The CD spectrum of renatured enzyme also demonstrated recovery of the single major peak at 208 nm characteristic of native enzyme. This property suggests that it will be feasible to perform flavin substitution experiments as a means of probing the chemistry at the active site.

Table 3: Solvent Deuterium Isotope Effects on Ligand Binding[a]

	pH 7.5	pH 8.0	pH 8.5
	$NADP^+$		
$^{H}K_d$ (μM)	2.0 ± 0.2	1.10 ± 0.11	1.1 ± 0.2
$^{D}K_d$ (μM)	1.6 ± 0.2	1.06 ± 0.12	0.5 ± 0.2
$^{H}K_d/^{D}K_d$	1.3 ± 0.2	1.04 ± 0.16	2.2 ± 1
	UNAGEP		
$^{H}K_d$ (μM)	3.6 ± 0.3	4.5 ± 0.3	8.1 ± 0.4
$^{D}K_d$ (μM)	1.8 ± 0.3	1.9 ± 0.2	2.1 ± 0.3
$^{H}K_d/^{D}K_d$	2.0 ± 0.4	2.4 ± 0.3	3.9 ± 0.6

[a] Binding titrations were performed as described in Materials and Methods at 20 °C. Three titrations in H_2O and three in D_2O were conducted at a single pH on the same day with the same enzyme sample. The final D_2O content was 94% in the D_2O titrations. Data for the three titrations in H_2O at a single pH were pooled and fitted to eq 2. Data for the three titrations in D_2O at a single pH were treated the same way. Data in the table correspond to the data in Figure 11.

In conjunction with the refolding experiment, the visible CD spectra of oxidized and reduced enzyme were obtained. These spectra showed conversion of the three negative Cotton peaks in the oxidized form to a single positive peak in the reduced form. More significantly, binding of UNAGEP and $NADP^+$ produced major changes in the visible CD signals of the flavin. Previous kinetic studies have suggested that UNAGEP binds to the oxidized form and that $NADP^+$ is a noncompetitive inhibitor, but these are the first experiments to demonstrate direct binding. Furthermore, the peak shifts exhibited upon UNAGEP or $NADP^+$ binding may be an indication that the redox potential of the flavin changes in the substrate-bound state (Edmondson & Tollin, 1971). Crystallographic studies have demonstrated structural differences in the UNAGEP bound and unbound states (Benson et al., 1996), and these structural differences may be the cause of the spectral shifts, and potentially may result in changes in the redox potential. Additional redox titrations will be necessary to determine the potential of the flavin in this system and to determine whether or not, or to what extent, substrate binding alters the redox potential. These measurements will be important in assessing the extent to which binding energy may be translated into catalytic efficiency.

The visible spectra in Figures 4 and 5 confirm that oxidized UNAGEP reductase binds both UNAGEP and $NADP^+$ in dead-end complexes. Binding results in a 10-nm red shift of the flavin peak from 464 to 474 nm and produces unique isosbestic points (at 380 and 410 nm for UNAGEP binding; at 378 and 406 nm for $NADP^+$ binding) and unique extinction coefficients (at 380 nm for UNAGEP binding; at 384 nm for $NADP^+$ binding). The well-defined isosbestic points provide evidence that a single complex forms during the titration (Connors, 1987). The slight differences in the isosbestic points indicate that the ligands generate similar but slightly different environments around the flavin when they bind. This is consistent with the changes in the CD spectra, which indicate clearly that the environment around the flavin has changed in a unique way for each ligand.

Very similar changes in the visible flavin spectrum have been observed upon ligand binding to other flavoenzymes. For example, wild-type lipoamide dehydrogenase exhibits no spectral change on β-NAD^+ binding, but a K53R mutant exhibits spectral shifts almost identical to those in Figures 4 and 5 (Maeda-Yorita et al., 1994). Also, *p*-hydroxybenzoate hydroxylase demonstrates a substrate-induced red shift involving an active-site arginine (van Berkel et al., 1992). The similarity of the spectral shifts in UNAGEP reductase to those in lipoamide dehydrogenase and *p*-hydroxybenzoate hydroxylase suggested that similar positive charge interactions might be present in UNAGEP reductase. In fact, the crystal structure of UNAGEP reductase, with UNAGEP bound, positions arginine 214 in the active site approximately 4 Å from the flavin N5. Arginine 214 forms a hydrogen bond with O4 of the FAD and is close enough to N5 that it might form a hydrogen bond to N5 after transfer of a hydride from NADPH (Benson et al., 1995). A second arginine, arginine 159, is within hydrogen-bonding distance of the O1B of UNAGEP and has been suggested to be a likely participant in transition-state stabilization (Benson et al., 1995). However, the hypothesis that either or both of these arginines might provide positive charges that modulate the spectrum of FAD in the presence of ligands must await spectroscopic analysis of site specific mutants.

The data in Table 2 show that for UNAGEP the K_d is 2.7 μM, the K_m is 2.2 μM, and the K_i due to substrate inhibition is 880 μM. Substrate inhibition arises from formation of the dead-end complex between E_{ox} and UNAGEP, for which the K_d is 2.7 μM. However, the K_i of 880 μM suggests that the interaction is much weaker. Clearly, K_d is a direct measure of the tightness of the E_{ox}·UNAGEP complex, wheras K_i was determined from a UNAGEP saturation profile in the presence of excess NADPH. Previously, we showed that UNAGEP is a competitive substrate inhibitor with respect to NADPH (Dhalla et al., 1995). Thus, the high K_i for UNAGEP in Table 2 is due to the fact that it was effectively competed out by NADPH. In other experiments, where UNAGEP and NADPH both were systematically varied and the pooled data were fitted globally to a rate equation for the entire mechanism (Dhalla et al., 1995), the K_i was 73 μM. This more accurately reflects the tightness of binding. Results from the kinetic saturation profile, the systematic variation of both substrates in kinetic profiles (Dhalla et al, 1995), and the direct titration data all provide a nice illustration of the fact that steady-state data reflect the complete set of rate constants for the mechanism but that direct binding experiments provide a measure of the true K_d.

Many flavoenzymes have been observed to stabilize a radical intermediate during anaerobic reductive titrations. In some cases, the radical may represent a chemically significant species during catalysis, whereas, in other cases, the radical cannot be observed under catalytic conditions and is not thought to be a reactive intermediate. However, no spectral evidence for a radical in the anaerobic reductive titrations of UNAGEP reductase was obtained. Anaerobic reduction with dithionite was complete at 1 equiv, and no long-wavelength absorbance peaks were observed that might suggest a flavin semiquinone. Similarly, reduction by NADPH and photochemical reduction produced no spectral peaks resembling a semiquinone. Reduction by NADPH also was essentially complete at 1 equiv. The stoichiometric reduction by dithionite and NADPH demonstrates that there are no other intermediate electron donors and that direct reduction of the flavin occurs from NADPH. Lack of evidence for a radical intermediate in the reductive titrations is consistent with classification of the enzyme as a carbon−carbon transhydrogenase (Massey & Hemmerich, 1980).

The featureless long-wavelength absorbance above 536 nm exhibited upon NADPH reduction is similar to that observed for pyridine nucleotide transhydrogenase (van den Broek & Veeger, 1971). This type of spectral absorbance suggests the formation of a charge transfer complex between the pyridine nucleotide and FAD. Similar featureless long-wavelength absorbance was observed during $NADP^+$ reoxidation of reduced enzyme.

Reoxidation of photochemically reduced enzyme by UNAGEP and $NADP^+$ differed dramatically. Titration of reduced enzyme with UNAGEP resulted in stoichiometric reoxidation, whereas titration with >25 equiv of $NADP^+$ did not. These results indicate that the first reductive half-reaction is in chemical equilibrium but that the second oxidative half-reaction greatly favors product formation.

Binding experiments with UNAGEP and $NADP^+$ in H_2O and D_2O demonstrated a significant solvent deuterium isotope effect on UNAGEP binding and to a lesser degree a solvent isotope effect on $NADP^+$ binding at pH 8.5. The pH maximum for enzyme activity is ≈8.0, and therefore the pH (pD) range for these experiments was chosen to cover a large portion of the enzymatically relevant pH range. Titrations were not performed at pH values below 7.5 because protein instability was observed near pH 7.0, as manifested by increased light scattering and precipitation (results not shown). The large solvent deuterium isotope effect on UNAGEP binding suggests that significant hydrogen bonding or full protonation in the enzyme-substrate complex stabilizes ground-state binding to E_{ox}. The E_{ox}·UNAGEP complex is a nonproductive complex. However, the interactions stabilizing this complex will be substantially the same as those stabilizing the productive E_{red}·UNAGEP complex, since the only difference is the hydride at N5 of the flavin.

Kinetic and crystallographic studies suggest that the enolpyruvyl moiety of the substrate may be the locus of the solvent dueterium isotope effect on UNAGEP binding. The enzyme is highly specific for UNAGEP, and the substrate analog lacking the enolpyruvyl moiety binds very poorly, with a K_{is} from kinetic experiments of 5.7 mM against UNAGEP as the varied substrate (Dhalla et al., 1995). The K_{is} of 5.7 mM contrasts with the K_d of 2.7 μM and the K_m of 2.2 μM for UNAGEP. Thus the enolpyruvyl moiety provides significant ground state binding interactions. This is consistent with the crystal structure of the enzyme−substrate complex, which shows that the carbonyl oxygen of the enolpyruvyl moiety may hydrogen-bond to Arg159 and/or Glu325 and that the negatively charged carboxylate oxygen in the enolpyruvyl moiety may hydrogen-bond to the backbone amide hydrogen of Ser229 or to a water molecule in the active site (Benson et al., 1995). These residues also have been proposed to participate in stabilization of a carbanion intermediate (Arg159 and Glu325) and to participate in the final protonation that produces product (Ser229) (Benson et al. 1995).

Given the significance of these residues in the crystal structure and the importance of the enolpyruvyl moiety for binding, the observed solvent deuterium isotope effect on

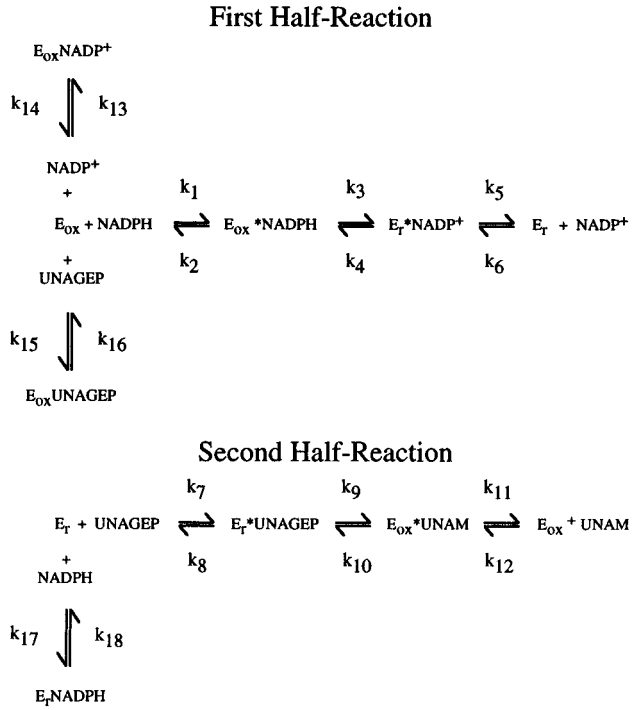

FIGURE 12: Kinetic model for the reaction catalyzed by UNAGEP reductase.

UNAGEP binding might well be rationalized as involving one or more of these protons. This would further imply that a solvent kinetic isotope effect might be significant on the reduction of the substrate vinylic bond, assuming that this step is cleanly rate-determining and isotopically sensitive. Moreover, a double isotope effect involving NADPD and solvent deuterium might be observed for reduction of the vinylic bond, but the identity of the solvent-derived deuterium atom would remain ambiguous due to the number of protons possibly involved in stabilization of the intermediate.

The titrations of oxidized enzyme with NADPH, $NADP^+$, and UNAGEP all demonstrated measurable spectral changes. Thus, a minimal first half-reaction can be described by a series of binding and chemical steps as shown in Figure 12. This is similar to the first half of the ping-pong bi-bi double competitive substrate inhibition mechanism previously proposed (Dhalla et al., 1995), except that an additional reaction for $NADP^+$ binding has been added to account for the results obtained in Figure 5. Previous kinetic experiments have shown that $NADP^+$ is a noncompetitive inhibitor with respect to NADPH. This indicates either that $NADP^+$ binds to two forms of the enzyme or that it can reverse the first half-reaction, or both. In fact, the results in Figures 5 and 9 demonstrate that $NADP^+$ does bind to two forms of the enzyme, the oxidized and reduced forms, and that binding to the reduced form can reverse partially the first half-reaction. Reoxidation of reduced enzyme by $NADP^+$ indicates that the k_3/k_4 and k_5/k_6 ratios represent reversible rather than irreversible steps. The steps represented by k_{13}/k_{14} and k_{15}/k_{16} also represent reversible steps, otherwise the data in Figures 5 and 6 would yield very tight binding constants, whereas in fact the binding constants were in the range of 0.7−2.0 μM.

However, the data obtained here provide no direct evidence that the step represented by k_1/k_2 is reversible, since >25 equiv of $NADP^+$ did not regenerate the fully oxidized spectrum. The spectra in Figure 9 clearly represent reoxidized enzyme, but whether they represent E_{ox}·NADPH or a mixture of E_{ox} and E_{ox}·NADPH has not been resolved. The long-wavelength absorption in Figure 9, characteristic of a charge transfer complex, suggests that the partially reoxidized spectra represent E_{ox}·NADPH. Thus, starting with E_{red}, once $NADP^+$ binds the redox potential of the flavin and pyridine nucleotide are more evenly matched and reoxidation occurs. This suggests that the chemical step, k_3/k_4, equilibrates between oxidation and reduction. Kinetically, however, the balance of the pathway from k_1/k_2 through k_3/k_4 and k_5/k_6 lies in the forward direction, since NADPH reduction is essentially stoichiometric in Figure 8 and the reverse reaction is incomplete with >25-fold excess of $NADP^+$. This would indicate that the reverse rates, k_2, k_4, and k_6, are slower than the forward rates and that k_2 may be negligible. Additional redox and potentiometric studies will have to be conducted to quantitate the magnitude of the redox potential with physiological substrates and with direct electron donors.

The second half-reaction in Figure 12 partitioned completely in the forward direction under all experimental conditions in this study. No evidence was obtained that UNAM can bind or reduce oxidized enzyme at concentrations up to 2 mM. In previous steady-state kinetic experiments, UNAM was found to be an uncompetitive inhibitor with respect to NADPH, with a K_i of 8.4 mM, which is >3000 times the binding constant of UNAGEP (Dhalla et al., 1995). Thus, at high enough concentrations, some UNAM binding does occur. Since we did not detect binding to E_{ox} spectroscopically, and binding to E_{ox} would result in competitive inhibition with respect to NADPH, the results imply that UNAM binds to E_{red} at high concentrations and that k_{12} is negligible. However, since there is no visible flavin signal for E_{red} it was not possible to look for UNAM binding to E_{red} directly. Therefore, since binding could not be confirmed directly and the K_i is very weak, UNAM binding does not contribute significantly to the kinetics of the overall reaction and a separate step for UNAM binding to E_{red} was not included in the kinetic mechanism in Figure 12.

For the second half-reaction, flavin reoxidation does provide a signal for estimation of rates k_7, k_9, and k_{11}, but one or more of the reverse rates k_8, k_{10}, and k_{12} appear to be negligible, and the step represented by k_{17}/k_{18} has no separate visible spectroscopic signal. However, the model includes a step for NADPH binding to E_{red}, even though no spectral signal was found for k_{17}/k_{18}, in order to account for the clear substrate inhibition observed previously (Dhalla et al., 1995). Finally, the model in Figure 12 represents a minimal mechanism for the kinetic steps catalyzed by UNAGEP reductase. Evidence indicates that chemical conversion of UNAGEP to UNAM may occur through stabilization of a carbanion intermediate (Benson et al., 1995), and thus product formation most likely occurs in two steps, rather than one as depicted in Figure 12. Whether or not these can be distinguished kinetically, however, has yet to be determined. Moreover, the model assumes no isomerization steps, though there are differences between the crystal structures of the substrate-bound and substrate-free forms of the enzyme that imply a signficant conformational change upon ligand binding (Benson et al., 1996).

In summary, these studies have defined the available spectroscopic signals for measurement of the microscopic steps in the kinetic mechanism and have shown that the two

half-reactions can be studied separately. The data also have shown that the first half-reaction is reversible but that the second half-reaction is irreversible under accessible experimental conditions. Furthermore, the enzyme can be reversibly unfolded and refolded with full reincorporation of FAD. This property makes it feasible to conduct flavin substitution experiments with flavin analogs to understand the redox properties of the enzyme. With the defined spectroscopic signals, it will now be possible to conduct transient-state kinetic experiments to define the microscopic rate constants.

ACKNOWLEDGMENT

We thank Dr. John Emanuele, Jr. for many valuable discussions of flavoenzyme properties and experimental techniques and Drs. Terry Stouch and Steven Sheriff for many valuable discussions of the crystal structure of UNAGEP reductase. We also thank Dr. Jiri Novotny for the neural network analysis of the protein sequence and Dr. Adil Dhalla for valuable comments on this work.

REFERENCES

Anderson, K. S., Sikorski, J. A., & Johnson, K. A. (1988) Evaluation of 5-Enolpyruvoylshikimate-3-phosphate Synthase Substrate and Inhibitor Binding by Stopped-Flow and Equilibrium Fluorescence Measurements, *Biochemistry 27*, 1604−1610.

Benson, T. E., Marquardt, J. L., Marquardt, A. C., Etzkorn, F. A., & Walsh, C. T. (1993) Overexpression, Purification, and Mechanistic Study of UDP-*N*-Acetylenolpyruvylglucosamine Reductase, *Biochemistry 32*, 2024−2030.

Benson, T. E., Walsh, C. T., & Hogle, J. M. (1994) Crystallization and Preliminary X-ray Crystallographic Studies of UDP-*N*-Acetylenolpyruvylglucosamine Reductase, *Protein Sci. 3*, 1125−1127.

Benson, T. E., Filman, D. J., Walsh, C. T., & Hogle, J. M. (1995) An Enzyme-Substrate Complex Involved in Bacterial Cell Wall Biosynthesis, *Nature Struct. Biol. 2*, 644−653.

Benson, T. E., Walsh, C. T., & Hogle, J. M. (1996) The Structure of the Substrate-Free Form of MurB, An Essential Enzyme for the Synthesis of Bacterial Cell Walls, *Structure, 4*, 47−54.

Bugg, T. D. H., & Walsh, C. T. (1992) Intracellular Steps of Bacterial Cell Wall Peptidoglycan Biosynthesis: Enzymology, Antibiotics, and Antibiotic Resistance, *Nat. Prod. Rep. 9*, 199−215.

Connors, K. A. (1987) Binding Constants and the Measurement of Molecular Complex Stability, p 143, John Wiley & Sons, New York.

Dhalla, A. M., Yanchunas, J., Jr., Ho, H.-T., Falk, P., Villafranca, J. J., & Robertson, J. G. (1995) Steady-State Kinetic Mechanism of *Escherichia coli* UDP-*N*-Acetylenolpyruvylglucosamine Reductase, *Biochemistry 34*, 5390−5402.

Edelhoch, H. (1967) Spectroscopic Determination of Tryptophan and Tyrosine in Proteins, *Biochemistry 6*, 1948−1954.

Edmondson, D. E., & Tollin, G. (1971) Circular Dichroism Studies of the Flavin Chromophore and of the Relation Between Redox Properties and Flavin Environment in Oxidases and Dehydrogenases, *Biochemistry 10*, 113−123.

Fieller, E. C. (1954) Some Problems in Interval Estimation, *J. R. Statist. Soc. B16*, 175−185.

Kabsch, W., & Sander, C. (1983) Dictionary of Protein Secondary Structure: Pattern Recognition of Hydrogen-Bonded and Geometrical Features, *Biopolymers 22*, 2577−2637.

Maeda-Yorita, K., Russell, G. C., Guest, J. R., Massey, V., & Williams, C. H., Jr. (1994) Modulation of the Oxidation−Reduction Potential of the Flavin in Lipoamide Dehydrogenase from *Escherichia coli* by Alteration of a Nearby Charged Residue, K53R, *Biochemistry 33*, 6213−6220.

Manavalan, P., & Johnson, W. C., Jr. (1987) Variable Selection Method Improves the Prediction of Protein Secondary Structure from Circular Dichroism Spectra, *Anal. Biochem. 167*, 76−85.

Massey, V., & Hemmerich, P. (1980) Active-Site Probes of Flavoproteins, *Biochem. Soc. Trans. 8*, 246−257.

Pucci, M. J., Discotto, L. F., & Dougherty, T. J. (1992) Cloning and Identification of the *Escherichia coli murB* DNA Sequence, Which Encodes UDP-*N*-Acetylenolpyruvoylglucosamine Reductase, *J. Bacteriol. 174*, 1690−1693.

Rost, B., & Sander, C. (1993) Prediction of Protein Structure at Better than 70% Accuracy, *J. Mol. Biol. 232*, 584−599.

Rost, B., & Sander, C. (1994) Combining Evolutionary Information and Neural Networks to Predict Protein Secondary Structure, *Proteins: Struct., Funct., Genet. 19*, 55−72.

van Berkel, W., Westphal, A., Eschrich, K., Eppink, M., & DeKok, A. (1992) Substitution of Arg214 at the Substrate-Binding Site of *p*-Hydroxybenzoate Hydroxylase from *Pseudomonas fluorescens*, *Eur. J. Biochem. 210*, 411−419.

van den Broek, H. W. J., & Veeger, C. (1971) Pyridine−Nucleotide Transhydrogenase 4. Studies on the Reductive Mechanism of Transhydrogenase from *Azotobacter vinelandii*, *Eur. J. Biochem. 24*, 63−71.

BI962260S